Molecular Catalysis 445 (2018) 43–51

Contents lists available at ScienceDirect

Molecular Catalysis

journal homepage: www.elsevier.com/locate/mcat

Research paper

An insight on the influence of surface Lewis acid sites for regioselective C—H bond C_3-cyanation of indole using NH_4I and DMF as combined cyanide source over Cu/SBA-15 catalyst

Venu Boosa[a], Vishali Bilakanti[a], Vijay Kumar Velisoju[a], Naresh Gutta[a], Sreedhar Inkollu[b], Venugopal Akula[a,*]

[a] Catalysis Laboratory, Inorganic and Physical Chemistry Division, CSIR-Indian Institute of Chemical Technology, Hyderabad, 500 007, Telangana, India
[b] Department of Chemical Engineering, BITS Pilani Hyderabad Campus, Hyderabad, 500078, India

ARTICLE INFO

Article history:
Received 18 August 2017
Received in revised form 25 October 2017
Accepted 3 November 2017

Keywords:
Regioselective C_3-cyanation
Cu-SBA-15
Indole
Lewis acid
NH_4I-DMF-cyanaide source

ABSTRACT

The Cu dispersed on mesoporous SBA-15 has demonstrated the regioselective C—H bond C_3-cyanation of indoles by in-situ generation of —CN using DMF and NH_4I in presence of O_2. Pyridine adsorbed diffuse reflectance infrared spectroscopy (DRIFTS) results revealed that surface Cu^{2+} species are acting as Lewis acid sites in the in-situ generation of cyano- group for the synthesis of indole nitriles. A direct correlation between Cu metal surface area and the indole nitrile yields are established and the dual role of copper is substantiated by N_2O titration and XPS techniques. The 10 wt%Cu/SBA-15 demonstrated superior performance when compared to Pd, Ru supported on SBA-15. The 10 wt%Cu/SBA-15 catalyst showed consistent activity and selectivity after the 4th cycle.

1. Introduction

The derivatives of indole nitriles exhibit broad range of biological activities and they are present in many agrochemicals, dyes, pharmaceuticals and natural products as a backbone of their structural frameworks and are also widely used in organic synthesis [1]. Additionally, 3-cyanoindoles are key intermediates for the preparation of functional groups, such as aldehydes, amines, ketones, amidines, amides, tetrazoles and their carboxyl derivatives [2]. Notably, 3-cyanosubstituted indoles are core structures in many biologically active compounds currently being developed as estrogen receptor ligands, hepatitis C virus inhibitors, or therapeutic agents for cardiovascular diseases [3,4]. Aryl nitriles are generally prepared from classical organic transformations, such as Sandmeyer [5] and Rosenmund-von Braun reaction [6], which are pre-functionalized starting materials for the cyanation of aryldiazonium salts or aryl halides by stoichiometric amounts of CuCN. However, these reactions suffer from the toxic CuCN source at high temperature with prolonged times and also multiple procedures.

Recently, the transition-metal-catalyzed cyanation of aryl halides [7], borons [8] or mesylates provide a promising alternative to the cyanation reactions [9]. In these procedures, several cyano sources were employed e.g. metal cyanides (NaCN, KCN, CuCN, TMSCN, $K_4[Fe(CN)_6]$), BnCN, t-BuNC, electrophilic CN^+ reagents (NCTs, BrCN), and combined cyano sources (NH_4I/DMF, DMF, NH_4HCO_3/DMSO, TMEDA/$(NH_4)_2CO_3$). Metal cyanides are frequently used as cyanide sources in various organic transformations. Nevertheless, almost all these methods suffer from limitations. An important issue to be resolved is the high affinity of the cyanide ion for the transition metal, which often results in rapid deactivation of catalyst. Moreover, most of the cyano sources, in particular NaCN, KCN and CuCN have notorious toxicity. For example $Zn(CN)_2$ leads to heavy metal waste and Me_3SiCN is sensitive to moisture and easily liberates hydrogen cyanide. Although $K_4[Fe(CN)_6]$ is exceptionally nontoxic, its slow solubility in organic solvent limits its usage. Acetone cyanohydrins [10] would greatly decrease the utility of the aforementioned transformations. To this end, a number of CN-containing small organic molecules such as cyanohydrins [11], CH_3CN [12], as well as molecule without a CN group such as formamide [13], DMF [14] and nitromethane [15] have been shown to be effective CN sources for aromatic cyanation reactions. In addition, more complicated strategies for generating a CN group from combined sources have been reported to achieve aromatic cyanation reactions, e.g., DMF + NH_3 [16], DMF + NH_4I [17], DMF + NH_4HCO_3 [18,19]. However, the search for methods using safer and easy handling CN sources remains highly desirable. C—H

---

* Corresponding author.
E-mail address: akula.iict@gov.in (V. Akula).

http://dx.doi.org/10.1016/j.mcat.2017.11.007

activation of sp^2 centres presents unique challenges. Selective and direct cyanation of highly abundant C—H bonds of (hetero) arenes has emerged as a powerful tool to achieve atom and step economy in organic synthesis. Most of these processes involve either the use of expensive noble metals or non-eco-friendly reagents. Therefore, the development of inexpensive acidic metal catalysts for the selective cyanation of indoles has become a topic of interest.

In this investigation, SBA-15 has been chosen as the support material for various metals such as Cu, Ru, Pd and Ni are examined for the regioselective C_3-cyanation of indole. In the comparative analysis, Cu/SBA-15 demonstrated a better nitrile yield than the Ru/SBA-15, Ni/SBA-15 and Pd/SBA-15 catalysts thus showing economic viability of the catalyst. A significant amount of work on cyanation reactions has been reported by Chang and co-workers. They have used DMF and ammonia or ammonium salts as the combined ‘CN’ source to realize the cyanation of the carbon–hydrogen (heteroatom) bond [20]. Cyanation of aromatic halides by employing ammonium bicarbonate and DMF (or) DMSO as the combined ‘CN’ source was also achieved [18,20]. These methods for cyanation reactions involve the combined ‘CN’ source composed of DMF or DMSO which provides the ‘C’ unit of ‘CN’, while the ‘N’ unit comes from ammonia or ammonium salts. We have examined the cyanation of aromatic C—H bonds by using a combination of NH_4HCO_3 and DMSO as the ‘CN’ source over a Pd(II) on Mg–La mixed oxide [21]. Recently, we have explored supported copper catalyst for the cyanation of arenes using NH_4HCO_3 and *N*,*N*-dimethylformamide as a CN source [22]. Transition-metal-catalyzed direct C—H activation and functionalization has become a powerful tool in organic synthesis [23]. In particular, the building of C—C and C-heteroatom bonds directly from two simple carbon-hydrogen (C—H) bonds or C—H and H—Nu (Nu=B, O, N, S) bonds provides an unusually attractive pathway by virtue of its step economy, lower cost, and a decrease in waste production [24]. Jianbo Wang and co-workers reported the Pd-catalyzed cyanation using $K_4[Fe(CN)_6]$ as cyanating agent and selectively introduce a cyano group into the 3-position of indoles with high efficiency [25]. Khorshidi showed the selective 3-cyanation of indoles was achieved under Ru catalyst [26]. Chaitanya and Anbarasan demonstrated the Rh catalyzed cyanation of indoles [27]. Yang et al. reported the Lewis acid catalyzed direct cyanation of indoles [28]. Shen and co workers reported the Cu-catalyzed cyanation of indoles using acetonitrile as a cyano source [29].

In recent years, mesoporous silica materials have attracted the catalysis community because of mesoporous silica (SBA-15) exhibits interesting textural properties, such as thick framework walls, uniform-sized pores (4–30 nm), large specific surface areas (above 1000 $m^2 g^{-1}$), high thermal stability and diffusion limitations and is widely used as catalyst supports, drug delivery materials [30–32], SBA-15 supported metals have revealed excellent activity and stability of the catalytic oxidation of organic compounds [33,34] and catalytic transfer hydrogenation and cyclization [35]. Herein, we report SBA-15 supported Cu catalysts for the selective 3-cyanation of indole C—H bonds by using a combination of NH_4I and DMF as the ‘CN’ source in the presence of oxygen is an attractive, atom-economic and environmentally benign oxidant due to the fact that it is cheap, widely available (20vol% of air) and clean (only water as by-product) to provide indole nitriles in good yields (Scheme 1). The Cu loaded SBA-15 samples are characterized by BET-surface area, powder X-ray diffraction (XRD), H_2-temperature programmed reduction (H_2-TPR), NH_3-temperature programmed desorption (NH_3-TPD), transmission electron microscopy (TEM), N_2O pulse titration for Cu metal surface area, X-ray photoelectron spectroscopy (XPS), pyridine adsorbed diffuse reflectance Fourier transformed infrared spectroscopy (DRIFTS).

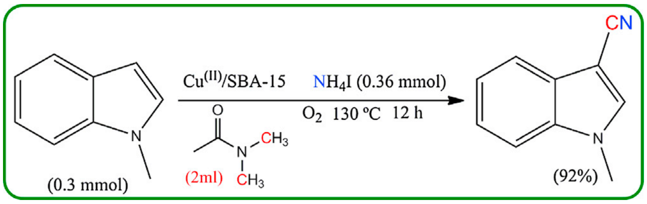

Scheme 1. Cyanation of *N*-methylindole.

2. Experimental section

2.1. Catalyst preparation

The mesoporous siliceous SBA-15 support was prepared according to the procedure reported by Zhao et al. [36]. In a typical method, using 2.0 g Pluronic P123 tri-block co-polymer surfactant dissolved in 15 g water, followed by the addition of 60 g of 2 M HCl. Under constant stirring, 4.25 g TEOS was added and the mixture was stirred continuously for 24 h at 40 °C. The gel mixture was then subjected to heat treatment in an autoclave at 100 °C for 48 h. After filtration, the obtained gel was dried in an air oven at 80 °C for 12 h. The dried SBA-15 solid was calcined in air flow at 550 °C for 8 h. The resultant mesoporous silica (SBA-15: conformed by powder XRD) was used as support. A series of copper loadings e.g. 2.5, 5, 7.5, 10 and 12.5 wt% were prepared by wet impregnation method using $Cu(NO_3)\cdot 3H_2O$ as copper precursor. The solid was dried in an oven at 100 °C for 12 h and subsequently calcined at 450 °C for 5 h in static air. The elemental analysis of prepared catalysts is investigated using atomic absorption spectroscopy and the results are listed in Table S1. The complete details on the characterization of the catalysts are given in Supporting Information.

2.2. Catalyst activity studies

A 10 mL round bottom flask was charged with *N*-methylindole (40 mg, 0.3 mmol), Cu/SBA-15 (150 mg), NH_4I (0.36 mmol), DMF (2 mL) and O_2 as oxidizing agent. The round bottom flask was kept for stirring at 130 °C. After 12 h of run, the reaction was monitored by TLC; 5 mL of ethyl acetate was added to the reaction mixture. The catalyst was separated by centrifugation followed by the treatment of the reaction mixture with 10 mL of brine solution. The organic layer is separated by ethyl acetate (3 × 5 mL). The combined ethyl acetate extract was dried with anhydrous Na_2SO_4 and it was concentrated under reduced pressure. The pure product was isolated by flash column chromatography on silica gel using ethyl acetate-hexane (3:1) as an eluent (pale yellow oil, 92% yield). The catalyst was washed with distilled water for several times then dried in an oven at 100 °C and used for the next cycle. Following the similar procedure the cyanation reaction was tested for 3 recycles.

3. Results and discussion

3.1. Powder X-ray diffraction (XRD)

The low angle XRD patterns of pure SBA-15 and Cu loaded SBA-15 samples are displayed in Fig. 1A. The XRD pattern of parent SBA-15 exhibited a well-resolved sharp intense diffraction peak at $2\theta = 0.8^\circ$ along with two other low intense peaks at $2\theta = 1.59^\circ$ and 1.8° corresponding to the (100), (110) and (200) reflections respectively which can be indexed to a mesoporous 2D hexagonal pore structure. However, there is no major change observed in the structure of SBA-15 in Cu loaded samples suggesting hexagonal structure is intact and stable.

Fig. 1B shows the wide angle XRD patterns of parent SBA-15 and calcined Cu/SBA-15 samples. The broad X-ray diffraction peak at

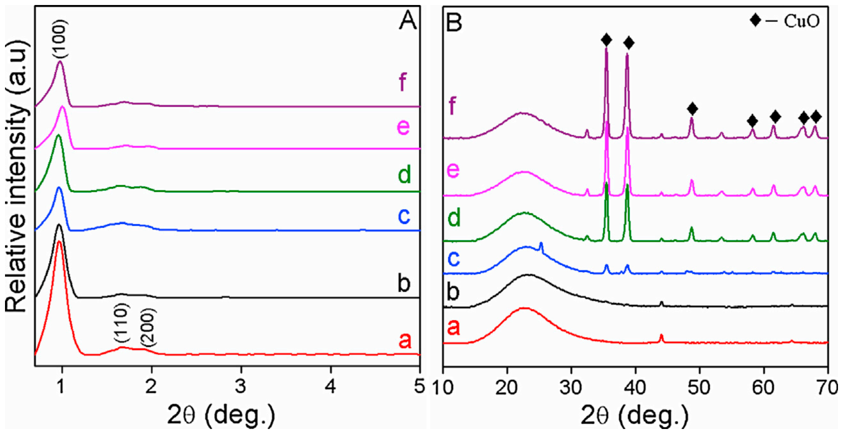

Fig. 1. (A) low angle and (B) wide angle XRD patterns of (a) 0.0 (b) 2.5 (c) 5.0 (d) 7.5 (e) 10.0 and (f) 12.5 wt%Cu supported on SBA-15.

$2\theta = 24^\circ$ corresponds to the presence of an amorphous silica phase. The XRD patterns exhibits that the diffraction signals of crystalline CuO are not formed at 5 wt% of Cu indicating the CuO species are present in a highly dispersed state at lower loading. At higher loading, the samples showed reflection at $2\theta = 35.5^\circ$ and 38.7° that are attributed to the crystalline CuO phase over the SBA-15 support. These diffraction peaks become sharper and intense with increase in Cu loading on SBA-15 (Fig. 1B) revealing that large size CuO clusters are formed.

3.2. *Physicochemical* ***characteristics*** *of the catalysts*

The N_2-sorption analysis of SBA-15 and copper loaded SBA-15 samples showed a high surface area for support material (Table 1), than on Cu loaded SBA-15. Upon increasing copper loading, a decrease in the surface area is however observed probably due to the pore blocking of the support material with the copper partices. The details on sorption isotherms (Fig. S1A), BJH analysis (Fig. S1B and Table S2) are reported in Supporting Information. The N_2O titration measurements are carried out and estimated the Cu metal suface area of the catalysts (Table 1). An increase in the N_2O uptake is observed with increase in copper loading and a higher Cu metal surface area is observed at a 10 wt% copper loading on SBA-15 (Table 1).

3.3. *H_2-temperature programmed reduction (H_2-TPR)*

The reducibility of the CuO particles interacted with SBA-15 investigated by using H_2-TPR analysis and profiles are presented in Fig. 2. The H_2-uptakes calculated (Table 1) from these curves showed an increase in the H_2 uptake with the increase in copper loading suggesting the bulk property of TPR analysis. The TPR profile of 2.5 wt%Cu/SBA-15 catalyst shows one main peak at 290 °C with a shoulder peak at 230 °C, which are attributed to bulk and finely dispersed CuO species respectively. When the copper loading increased from 2.5 to 10 wt%, the main reduction peak is shifted towards high temperature and become relatively broad. The TPR profile of 12.5 wt%Cu/SBA-15 sample exhibited typically two stage reduction, one around 270 °C which is ascribed to the reduction of finely dispersed CuO on the mesoporous SBA-15, while the reduction peak at 270–340 °C is probably due to the copper cluster interacted with SBA-15 support [37]. The broadening of the signal and the shift in T_{max} toward high temperature may be explained by the strong metal support interaction and formation of large clusters of CuO on the support.

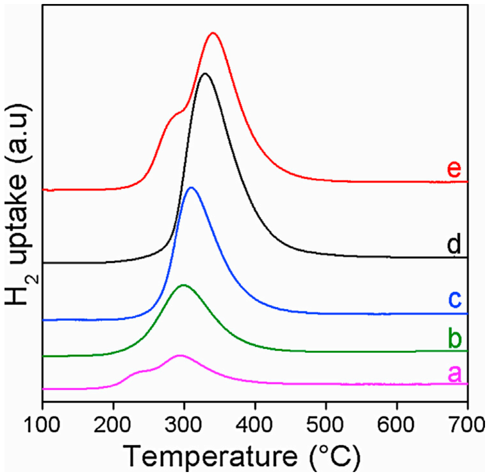

Fig. 2. H_2-TPR profiles of (a) 2.5, (b) 5.0, (c) 7.5, (d) 10 and (e) 12.5 wt%Cu supported on SBA-15.

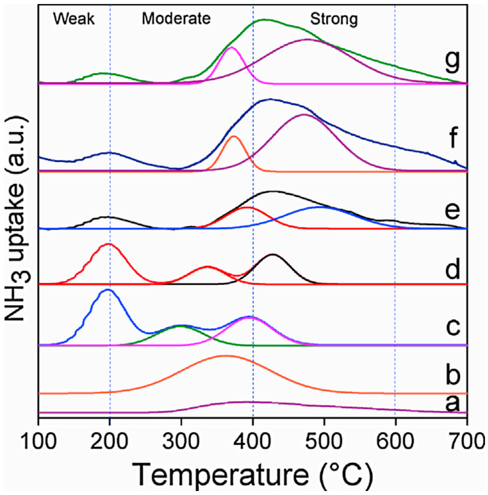

Fig. 3. NH_3-TPD profiles of (a) Pure SBA-15 (b) bulk CuO (c) 2.5 (d) 5.0 (e) 7.5 (f) 10 and (g) 12.5 wt%Cu supported on SBA-15 samples.

3.4. *NH_3-TPD analysis of the catalysts*

The acid site distribution on Cu supported on SBA-15 is classified based on the NH_3 desorption profiles as weak (<200 °C), medium (200–400 °C) and strong acidic sites (>400 °C) (Fig. 3) and the acid site distribution is given in Table S3. The bulk CuO has shown mostly

Table 1
Physicochemical characteristics of the catalysts.

Cu wt% on SBA-15	S_{BET} (m^2 g^{-1})[a]	H_2 uptake (μmol $g_{cat}{}^{-1}$)[b]	NH_3 uptake [c] mmol $g_{cat}{}^{-1}$	N_2O uptake/ (μmol $g_{cat}{}^{-1}$)[d]	[e]S_{Cu}/ m^2 $(g_{Cu})^{-1}$
0.0	639	nd	nd	nd	nd
2.5	568	248.3	0.51	13.8	45.2
5.0	476	392.6	0.62	35.4	57.9
7.5	425	463.2	0.74	67.2	73.4
10.0	393	578.9	0.96	111.6	91.4
12.5	385	729.6	0.92	129.6	84.9

[a] Determined from N_2-sorption analysis.
[b] Calculated from H_2-TPR using a calibrated Ag_2O TPR curve.
[c] Obtained from TPD of NH_3 analysis.
[d] Obtained from N_2O titration.
[e] Calculated using N_2O uptake by taking the Cu cross sectional area = 6.8×10^{-20} m^2 (Cu atom)$^{-1}$.

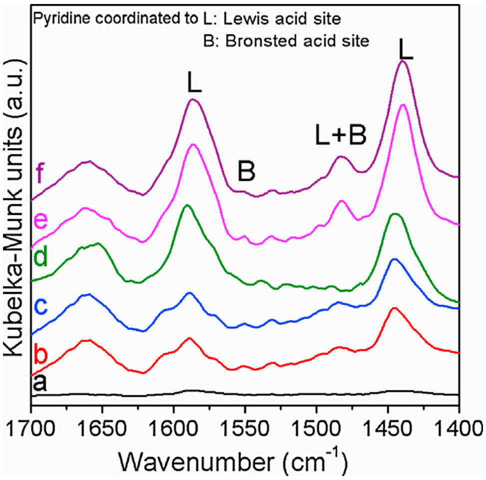

Fig. 4. Pyridine adsorbed DRIFT spectra of (a) 0.0 (b) 2.5 (c) 5.0 (d) 7.5 (e) 10 and (f) 12.5wt%Cu supported on SBA-15.

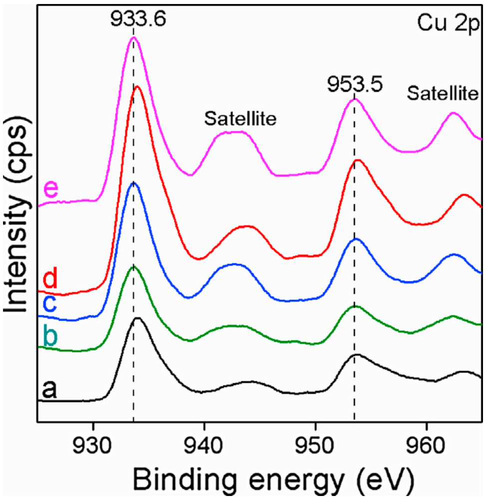

Fig. 5. The X-ray photoelectron spectra of (a) 2.5 (b) 5.0 (c) 7.5 (d) 10 and (e) 12.5 wt%Cu supported on SBA-15.

moderate acid sites which are probably Lewis acidic in nature. The NH_3 uptake is found to be low (~0.42 μmol $(g_{cat})^{-1}$) on bulk CuO when compared to the copper supported on SBA-15 samples (Table S3). The minute signal in the temperature region 300–500 °C is due to drift in the baseline as the SBA-15 is known to be a neutral support (Fig. 3a). The copper loaded SBA-15 samples exhibited 3 types of acidic sites on the surface. Upon increasing the copper loading on SBA-15 (Table 1), the surface acidity is enhanced which is explained due to acidic sites contributed from ionic copper species [38]. The TPD of NH_3 results demonstrated that a high ratio of moderate to strong acid sites are present in both 10 wt% and 12.5 wt% Cu/SBA-15 catalysts compared to lower loadings. For comparison, the TPD of NH_3 is also carried out for 10 wt%Cu/SiO_2, 10 wt%Cu/CeO_2 and 10 wt%Cu/MCM-41 catalysts in which at least 2 signals due to NH_3 desorption corresponding to weak and moderate acid sites are observed (Fig. S2).

3.5. *Pyridine adsorbed DRIFTS analysis*

The nature and type of acid sites (Lewis/Brønsted) present in the catalysts is examined using pyridine adsorbed FT-IR spectroscopy (Fig. 4). The normalized spectra showed vibrational bands in the range 1700–1400 cm^{-1} are assigned to both Brønsted and Lewis acid sites present on the surface of the catalyst according to the reported literature [39,40]. As shown in Fig. 4, it is evident that SBA-15 and Cu loaded SBA-15 catalysts showed mainly Lewis acid sites (co-ordinated pyridine: ~1450 and 1610 cm^{-1}) on the catalyst surface with minute amount of Brønsted acidity (protonated pyridine: ~1540 and 1640 cm^{-1}). Upon increasing the Cu loading from 2.5 to 12.5 wt%, an increase in the peak intensities are observed indicating high proportion of acid sites at higher loadings (i.e. 10 and 12.5 wt%). These results are consistent with the results obtained from TPD of NH_3 analysis (Fig. 3).

3.6. *Transmission electron microscopic (TEM) analysis*

The morphology of Cu/SBA-15 catalysts are analysed by TEM analysis. As shown in (Fig. S3), the 10wt%Cu/SBA-15 catalyst displays a 2D hexagonal structure of uniform mesoporous channels which are typical for SBA-15 type materials. This is in good agreement with the data obtained from the N_2-physisorption and XRD analysis where the preservation of silica structure after the copper is impregnated on it. It can be seen that the copper particles are well dispersed into the channels of SBA-15 and are stabilised by the silica support material (SBA-15) [41–43]. The TEM image of the used sample (recovered after the reaction) showed similar texture and morphology indicating the stability of the catalyst under the reaction conditions applied (Fig. S3).

3.7. *X-ray photo electron spectroscopic (XPS) analysis*

The fresh catalysts have been characterized by XPS analysis to investigate the Cu oxidation state and the chemical composition at the near surface region (Fig. 5). The binding energy values of Cu *2p*$_{3/2}$ O *1s* and Si *2p* (Fig. S4) are in good agreement with the reported values [22]. The Cu 2p spectra of the various Cu loaded SBA-15 samples, indicated two main signals at 933.6 and 953.5 eV attributed to $2p_{3/2}$ and $2p_{1/2}$ states of Cu^{2+} species. An increase in peak intensity is observed due to the high copper content in higher Cu loading catalysts (Table S4).

3.8. Activity measurements

Table 2 indicates the dependence of the cyanation activity over various loadings of copper on SBA-15 for the C—H bond cyanation of *N*-methylindole at 130 °C. The pure SBA-15 is found to be inactive for the formation of 3-cyanoindole product. The 3-cyanoindole formation is found to increase with increase in copper loading up to a 10 wt% and further increase in Cu loading to 12.5 wt% leads to no significant changes in the activity. These results therefore imply that the 10 wt%Cu loading on SBA-15 is an optimum composition, which established higher yields compared to other loadings on SBA-15.

Further the reaction parameters are optimized by using *N*-Methylindole as the model substrate. Using 150 mg of Cu/SBA-15 catalyst, a combination of NH_4I (0.36 mmol) and DMF (2 mL) as the cyanating agent and O_2 as oxidant; are used achieved 92% yield of the desired product i.e. 3-cyano-1-methylindole (Table 3, entry 1). Under similar experimental conditions, using DMSO as the cyanating agent, lower yield of the product is obtained compared to DMF (Table 3, entry 2). When DMF is used in presence of H_2O, 40% yield is obtained (Table 3, entry 3) and no activity towards the desired product is observed using acetonitrile (CH_3CN) as the cyanating agent (Table 3, entry 4). From these results it is evident that DMF is a suitable "C" source for the 3-cyanoindole reaction. The influence of oxidizing agent is investigated by employing different oxidizing agents such as TBHP, Ag_2O and H_2O_2 which were found to show low activity compared to O_2 as oxidizing agent (Table 3, entry 5, 6 and 7). When O_2 is replaced with under N_2 atmosphere, very low yield (15%) of the product observed is observed (Table 3, entry 8). These results thus indicate that O_2 is a suitable green oxidant for the 3-cyanoindole reaction. No activity towards the desired product is observed when the "N" source of NH_4I is replaced with NH_4OAc and/or NH_4Cl (Table 3, entry 9, 10). In presence of the aq. NH_3 solution, the catalyst displayed poor yield (40%) of the product (Table 3, entry 11). When the reaction is carried out in the absence of "N"; reaction did not take place (Table 3, entry 12). Therefore, these results reveal that the presence of NH_4I is necessary to get the desired product. In summary, the above findings of the cyanation reaction suggest that an array of DMF and NH_4I are feasible 'CN' source for this cyanation reaction in combination with O_2 as oxidizing agent.

In the absence of copper, no selectivity towards the desired product is observed over SBA-15 as catalyst (Table 3, entry 13). In order to see the support role, different supports are also used for copper such as HAP, Al_2O_3, SiO_2, Mg-LaO, CeO_2 and MCM-41 and tested for the cyanation reaction (Table 3, entry 14–19). However, the results revealed no improved yields of the desired product over these catalysts compared to Cu/SBA-15; thus suggesting the SBA-15 as suitable support for Cu in the cyanation of *N*-methylindole reaction. Furthermore, the influence of metal is also investigated using the other metals such as Ni, Pd and Ru on SBA-15 and the results of this analysis revealed inferior activity towards the desired product compared to Cu/SBA-15 catalyst (Table 3, entry 20–22). Finally, the superior performance of copper based catalyst towards the desired product (i.e. 3-cyano-*N*-methylindole) compared to Ru, Pd and/or Ni supported on SBA-15 catalysts may possibly explained by a higher rate of redox cycle on Cu/SBA-15 under the experimental conditions adopted.

The influence of reaction temperature is also checked for this reaction under the optimized experimental conditions. At room temperature, no cyanation product formation is observed over the 10 wt%Cu/SBA-15 catalyst (Table 3, entry 23). When the reaction temperature is increased from 80 °C to 130 °C, an increase in the yield of cyanation product is observed (Table 3, entry 1, 24–25) and further increase in temperature to 140 °C, no significant change in catalytic activity is found (Table 3, entry 26). The reaction time has also influenced the catalytic activity and formation of desired product. At 5 h of reaction time, the yield of product is 25% (Table 3, entry 27). Further increase in reaction time to 16 h, an improved yield (60% and 95%) of the product is observed (Table 3, entry 28 and 29). The 10 wt%Cu/SBA-15 has been examined at a higher substrate loading of 2 mmol with ~1 g of catalyst that showed excellent yield (89%) towards the desired compound without byproduct formation (Table 3, entry 30). We have eliminated the ambiguity related to the influence of other Lewis acid catalyst by testing the activity over α-AlF_3 under similar experimental conditions. Using the solid Lewis acid catalyst i.e. α-AlF_3 no activity (Table 3, entry 31) towards the desired product was observed; emphasizing the prominent role of Cu^{2+} in the in situ generation of —CN group and subsequent formation of indole nitriles. In-situ generation of —CN group has also been confirmed using TLC test, which is also cross checked with the cyanide ion identification test reported by Chahal and Sankar [44].

The influence of Cu^{2+} species for this reaction is also carried out over Cu(II) salts such as $CuCl_2\ 2H_2O$ and $Cu(NO_3)_2\ 3H_2O$ which showed about 22 and 18% yields towards the desired product respectively (Table 3, entries 32 and 33). These results thus indicating the bulk Cu^{2+} species are not much effective for the C_3-cyanation of indoles when compared to the copper dispersed on SBA-15 catalysts.

4. Substrate scope

The substituted indoles were subjected to the optimized reaction conditions and the results are illustrated in Fig. 6. The reaction can be utilized for cyanation of substituted indoles. The regioselectivity towards the C_3-cyanation products were exclusively observed in electron rich and electron deficient substituent on indole rings. It is observed that electron-rich group substituted substrates reacted more efficiently than electron-deficient group substituted substrates which is consistent with the rule of electrophilic iodination of indoles. The substrates bearing methyl (-Me) groups furnished the desired 3-cyanaindoles 69% and 65% yields (Fig. 6b and Fig. 6c). To some extent, the reaction is sensitive to methoxy substitution on the 4th position of the indole ring (Fig. 6d), delivering the product in a slightly lower yield than its 5th position of counterpart (Fig. 6e). The reaction of substrates with halogen analogues (F and Cl) performed smoothly to the expected 3-cyanoindole product 72% and 70% yields respectively (Fig. 6f and g). In contrast, the electron withdrawing substituent such as $-NO_2$ (Fig. 6h), −CN (Fig. 6i) and −COOMe (Fig. 6j) were compatible under standard reaction conditions to obtain desired 3-cyanoindoles with moderate yields of 65%, 63% and 50%respectively. Noteworthy, by changing substituent on the nitrogen atom, we found that 1H indole with free 'NH' did not show any activity towards the desired product (Fig. 6k). Interestingly, the substrates with ethyl and benzyl groups (Fig. 6l), (Fig. 6m) on the 'N' atom led to cyanation process produced good yields 73% and 65% respectively. When the 2nd position of indole is occupied by a phenyl group substrate (Fig. 6n), the cyanation reaction with corresponding cyano derivatives of indole showed very good yield of 70%. Particularly, the heteroaryl indoles could be successfully converted to the desired product in 55% yield (Fig. 6o).

4.1. Reaction mechanism for N-methylindole cyanation

Based on the obtained data using various substrates under optimized conditions a plausible mechanism for the cyanation reaction is illustrated in Scheme 2. The reaction proceeds via two sequen-

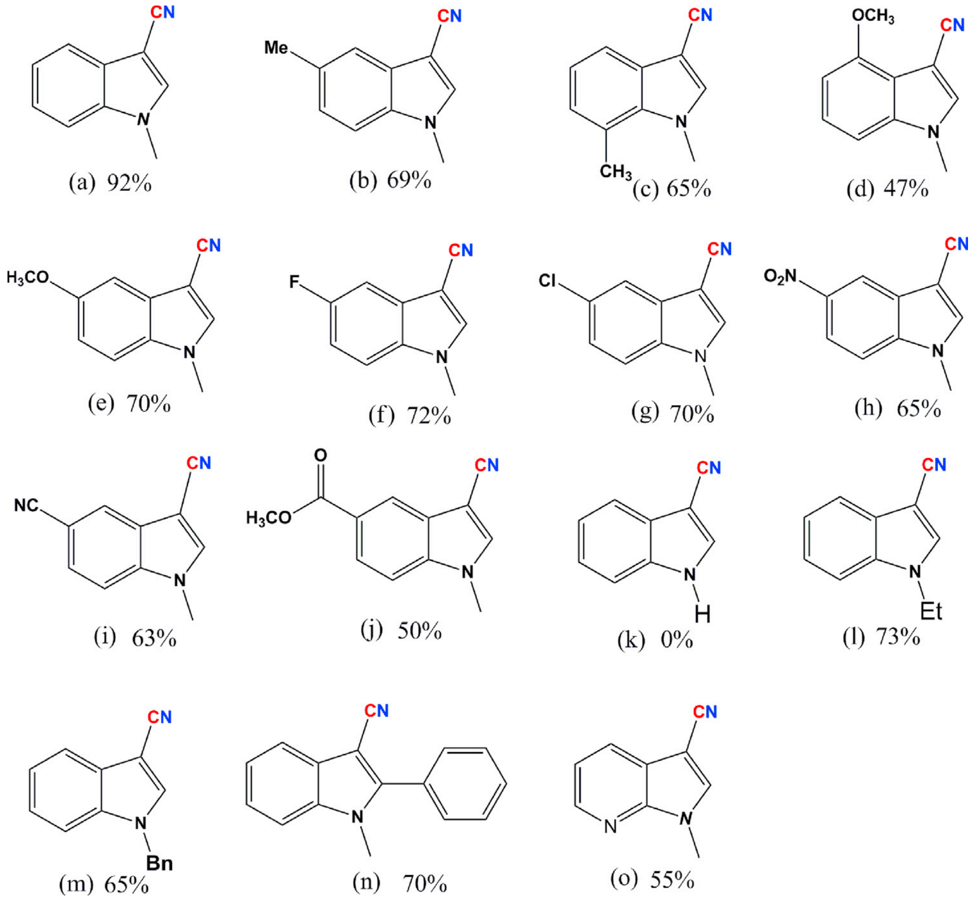

(a) 92%
(b) 69%
(c) 65%
(d) 47%
(e) 70%
(f) 72%
(g) 70%
(h) 65%
(i) 63%
(j) 50%
(k) 0%
(l) 73%
(m) 65%
(n) 70%
(o) 55%

Fig. 6. Cyanation of substituted indoles catalyzed by 10 wt%Cu/SBA-15.

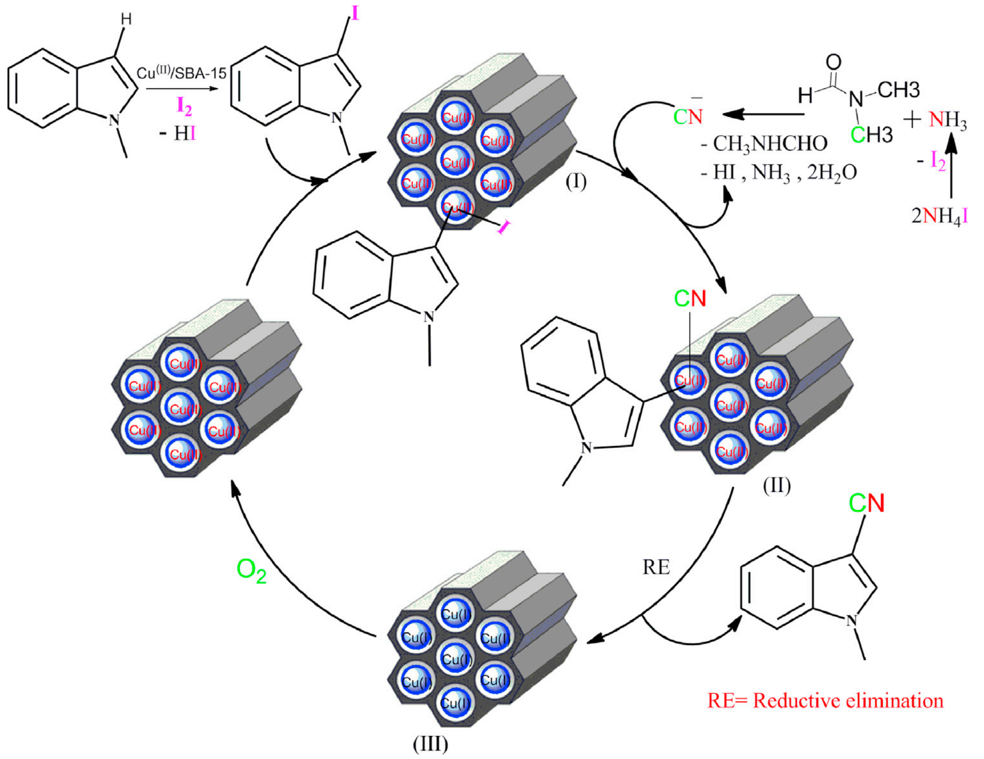

Scheme 2. Plausible reaction mechanism for C (SP^2)-H Cyanation over Cu/SBA-15 catalysts.

Table 2
Influence of copper loading on SBA-15 for cyanation activity.

Entry	Substrate	Catalyst	Oxidant	N source	Solvent	Yield (%)
1	*N*-Methylindole	SBA-15	O_2	NH_4I/0.36	DMF	0.0
2	*N*-Methylindole	2.5 wt%Cu/SBA-15	O_2	NH_4I/0.36	DMF	30
3	*N*-Methylindole	5.0 wt%Cu/SBA-15	O_2	NH_4I/0.36	DMF	47
4	*N*-Methylindole	7.5 wt%Cu/SBA-15	O_2	NH_4I/0.36	DMF	65
5	*N*-Methylindole	10 wt%Cu/SBA-15	O_2	NH_4I/0.36	DMF	92
6	*N*-Methylindole	12.5 wt%Cu/SBA-15	O_2	NH_4I/0.36	DMF	95

Reaction conditions: *N*-Methylindole (0.3 mmol), NH_4I (0.36 mmol), 150 mg of Cu/SBA-15 catalyst, DMF (2 mL), Oxidant (O_2 balloon) at 130 °C for 12 h.

Table 3
Optimization of reaction parameters for the cyanation *N*-methylindole.

Entry	Substrate	Catalyst	Oxidant	N source	Solvent	Yield (%)
1	*N*-Methylindole	10 wt%Cu/SBA-15	O_2	NH_4I/0.36	DMF	92
2	*N*-Methylindole	10 wt%Cu/SBA-15	O_2	NH_4I/0.36	DMSO	70
3	*N*-Methylindole	10 wt%Cu/SBA-15	O_2	NH_4I/0.36	DMF + H_2O	40
4	*N*-Methylindole	10 wt%Cu/SBA-15	O_2	NH_4I/0.36	CH_3CN	0.0
5	*N*-Methylindole	10 wt%Cu/SBA-15	H_2O_2	NH_4I/0.36	DMF	35
6	*N*-Methylindole	10 wt%Cu/SBA-15	TBHP	NH_4I/0.36	DMF	30
7	*N*-Methylindole	10 wt%Cu/SBA-15	Ag_2O	NH_4I/0.36	DMF	10
8	*N*-Methylindole	10 wt%Cu/SBA-15	N_2	NH_4I/0.36	DMF	15
9	*N*-Methylindole	10 wt%Cu/SBA-15	O_2	NH_4Cl	DMF	0.0
10	*N*-Methylindole	10 wt%Cu/SBA-15	O_2	NH_4OAC	DMF	0.0
11	*N*-Methylindole	10 wt%Cu/SBA-15	O_2	$NH_{3(aq)}$	DMF	40
12	*N*-Methylindole	10 wt%Cu/SBA-15	O_2	–	DMF	0.0
13	*N*-Methylindole	SBA-15	O_2	NH_4I/0.36	DMF	0.0
14	*N*-Methylindole	10 wt%Cu/HAP	O_2	NH_4I/0.36	DMF	30
15	*N*-Methylindole	10 wt%Cu/Al_2O_3	O_2	NH_4I/0.36	DMF	10
16	*N*-Methylindole	10 wt%Cu/SiO_2	O_2	NH_4I/0.36	DMF	30
17	*N*-Methylindole	10 wt%Cu/CeO_2	O_2	NH_4I/0.36	DMF	40
18	*N*-Methylindole	10 wt%Cu/MCM-41	O_2	NH_4I/0.36	DMF	55
19	*N*-Methylindole	10 wt%Cu/Mg-LaO	O_2	NH_4I/0.36	DMF	0.0
20	*N*-Methylindole	10 wt%Ni/SBA-15	O_2	NH_4I/0.36	DMF	30
21	*N*-Methylindole	10 wt%Pd/SBA-15	O_2	NH_4I/0.36	DMF	70
22	*N*-Methylindole	10 wt%Ru/SBA-15	O_2	NH_4I/0.36	DMF	45
23[b]	*N*-Methylindole	10 wt%Cu/SBA-15	O_2	NH_4I/0.36	DMF	0.0
24[c]	*N*-Methylindole	10 wt%Cu/SBA-15	O_2	NH_4I/0.36	DMF	40
25[d]	*N*-Methylindole	10 wt%Cu/SBA-15	O_2	NH_4I/0.36	DMF	68
26[e]	*N*-Methylindole	10 wt%Cu/SBA-15	O_2	NH_4I/0.36	DMF	94
27[f]	*N*-Methylindole	10 wt%Cu/SBA-15	O_2	NH_4I/0.36	DMF	25
28[g]	*N*-Methylindole	10 wt%Cu/SBA-15	O_2	NH_4I/0.36	DMF	60
29[h]	*N*-Methylindole	10 wt%Cu/SBA-15	O_2	NH_4I/0.36	DMF	95
30[i]	*N*-Methylindole	10 wt%Cu/SBA-15	O_2	NH_4I/0.36	DMF	89
31	*N*-Methylindole	α-AlF_3	O_2	NH_4I/0.36	DMF	0.0
32[j]	*N*-Methylindole	$CuCl_2$ $2H_2O$	O_2	NH_4I/0.36	DMF	22
33[j]	*N*-Methylindole	$Cu(NO_3)_2$ $3H_2O$	O_2	NH_4I/0.36	DMF	18

[a] Reaction conditions: *N*-Methylindole (0.3 mmol), N source (0.36 mmol), 0.150 g of 10wt%Cu/SBA-15 catalyst, Solvent (2 mL), Oxidant (O_2 balloon) at 130 °C for 12 h.
[b] Reaction at room temperature.
[c] Reaction at 80 °C.
[d] Reaction at 100 °C.
[e] Reaction at 140 °C.
[f] 5 h at 130 °C.
[g] 10 h at 130 °C.
[h] 16 h at 130 °C.
[i] Reaction at 130 °C for 12 h using *N*-Methylindole (2 mmol), catalyst: ~1.0 g.
[j] Copper salt amount: 0.150 g, *N*-Methylindole (0.3 mmol), N source (0.36 mmol), Solvent (2 mL), Oxidant (O_2 balloon) at 130 °C for 12 h.

tial steps: initial iodination followed by cyanation. In this reaction, ammonium iodide plays a dual role under the conditions employed: as a source of iodide for the formation of iodine molecule as well as a supplier of a nitrogen atom of the cyano unit. An electrophilic aromatic substitution is believed to be involved in the iodination of indoles to offer a 3-iodoindole intermediate. The *in situ* generated cyanide anion would subsequently take part in the cyanation of *N*-methylindoles and it forms the intermediate (II). The intermediate readily undergoes the reductive elimination process and provides the desired 3-cyano-*N*-methylindole product. Subsequent reductive elimination generates Cu(I) and it could be re-oxidized to Cu(II) by O_2 molecule to complete the catalytic cycle [1,45].

4.2. *Recyclability studies*

The recyclability of the catalyst is investigated over 10 wt%Cu/SBA-15 using *N*-methylindole, NH_4I and DMF at 130 °C that showed the consistent activity for three consecutive cycles (Fig. 7). In the recyclability process, the catalyst recovered by a simple centrifugation followed by washed with distilled water, dried at 100 °C for 12 h and used directly for the next cycle without any further purification. The used catalyst is also extensively characterized using XRD, XPS and ICP-OES analyses and compared with the characterizations of the fresh catalyst. It has been observed that no significant changes in the surface and bulk properties of the used catalyst compared to its fresh form

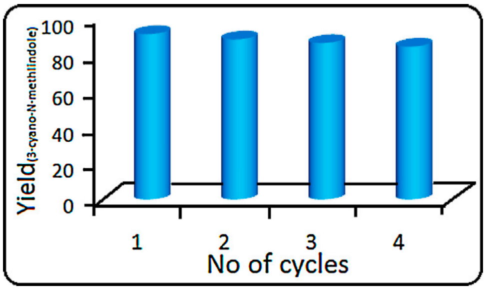

Fig. 7. Recyclability study over the 10 wt%Cu/SBA-15 catalyst.

suggesting that the 10 wt%Cu/SBA-15 is sustainable under the experimental conditions adopted in this study.

4.3. *Characterization of the used catalyst*

The used 10 wt%Cu/SBA-15 sample is characterized by using XRD and compared with its fresh form that showed no significant changes even after 4 cycles (Fig. S5). XPS analysis of the fresh and used 10 wt%Cu/SBA-15 catalyst further confirmed that there is no change in surface chemical composition and also binding energy of Cu 2p spectra even after 4 consecutive cycles (Fig. S6). The ICP-OES analysis of fresh and used (after 4th cycle) 10 wt%Cu/SBA-15 showed about 9.72% and 9.60 wt% of Cu respectively (Table S5), confirming that there is no leaching of Cu from the catalyst surface suggesting the robust nature of Cu/SBA-15 for the cyanation of indole compounds under the experimental conditions.

5. Conclusions

A simple copper impregnated SBA-15 system is examined for the cyanation of *N*-methylindole reaction. The 10 wt%Cu supported on SBA-15 demonstrated the superior performance in the cyanation reaction compared to other loadings. High ratio of Lewis acid sites and a high dispersion of copper are the key reasons for the high activity of 10 wt%Cu/SBA-15 catalyst. Under the optimized conditions; the Cu/SBA-15 catalyst for the cyanation reaction revealed that DMF as "C" source, NH_4I as "N" source and O_2 as oxidant are suitable for the high selectivity of the desired product at 130 °C. Based on product distribution, a reaction mechanism is proposed and discussed using the surface characteristics of the catalysts. The recyability results revealed that the 10 wt%Cu/SBA-15 catalyst sustained for the cyanation reaction and demonstrated stable activity even after 3 recycles under the experimental conditions maintained.

Acknowledgements

The authors Boosa Venu and Vishali Bilakanti thanks UGC New Delhi for the award of research fellowship.

Appendix A. Supplementary data

Supplementary data associated with this article can be found, in the online version, at http://dx.doi.org/10.1016/j.mcat.2017.11.007.

References

[1] M. Zhao, W. Zhang, Z. Shen, J. Org. Chem. 80 (2015) 8868–8873.
[2] K. Yamaguchi, N. Xu, X. Jin, K. Suzuki, N. Mizuno, Chem. Commun. 51 (2015) 100310037.
[3] S.A. Patil, R. Patil, D.D. Miller, Curr. Med. Chem. 18 (2011) 615–637.
[4] T.G. Murali Dhar, Z. Shen, H.H. Gu, P. Chen, D. Norris, S.H. Watterson, S.K. Ballentine, C.A. Fleener, K.A. Rouleau, J.C. Barrish, R. Townsend, D.L. Hollenbaugh, E.J. Bioorg Iwanowicz, Med. Chem. Lett. 13 (2003) 3557–3560.
[5] T. Sandmeyer, Chem. Ber. 17 (1884) 2650–2653.
[6] K.W. Rosenmund, E. Struck, Ber. Dtsch. Chem. Ges. 2 (1919) 1749–1756.
[7] (a) J. Zanon, A. Klapars, S.L. Buchwald, J. Am. Chem. Soc. 125 (2003) 2890–2891;
(b) M. Sundermeier, A. Zapf, M. Beller, Eur. J. Inorg. Chem. (2003) 3513–3526;
(c) S. Erhardt, V.V. Grushin, A.H. Kilpatrick, S.A. Macgregor, W.J. Marshall, D.C. Roe, J. Am. Chem. Soc. 130 (2008) 4828–4845;
(d) W. Zhou, J. Xu, L. Zhang, N. Jiao, Org. Lett. 12 (2010) 2888–2891;
(e) D.N. Sawant, Y.S. Wagh, P.J. Tambade, K.D. Bhatte, B.M. Bhanage, Adv. Synth. Catal. 353 (2011) 781–787;
(f) H. Yu, R.N. Richey, W.D. Miller, J. Xu, S.A. May, J. Org. Chem. 76 (2010) 665–668;
(g) A.V. Ushkov, V.V. Grushin, J. Am. Chem. Soc. 133 (2011) 10999–11005;
(h) M. Shevlin, Tetrahedron Lett. 51 (2010) 4833–4836.
[8] (a) Z. Zhang, L.S. Liebeskind, Org. Lett. 8 (2006) 4331–4333;
(b) C.W. Liskey, X. Liao, J.F. Hartwig, J. Am. Chem. Soc. 132 (2010) 11389–11391;
(c) G. Zhang, L. Zhang, M. Hu, J. Cheng, Adv. Synth. Catal. 353 (2011) 291–294;
(d) P. Anbarasan, H. Neumann, M. Beller, Angew. Chem., Int. Ed. 50 (2011) 519–522.
[9] P.Y. Yeung, C.M. So, C.P. Lau, F.Y. Kwong, Angew. Chem Int. Ed. 49 (2010) 8918–8922.
[10] (a) M. Sundermeier, A. Zapf, M. Beller, Angew. Chem Int. Ed. 42 (200) (1661-1664);
(b) E.J. Park, S. Lee, S. Chang, J. Org. Chem. 75 (2010) 2760–2762;
(c) T. Schareina, A. Zapf, A. Cotte, M. Gotta, M. Beller, Adv. Synth. Catal. 353 (2011) 777–780.
[11] K. Ouchaou, D. Georgin, F. Taran, Synlett (2010) 2083–2086.
[12] F.H. Luo, C.I. Chu, C.H. Cheng, Organometallics 17 (1998) 1025–1030.
[13] (a) D.N. Sawant, Y.S. Wagh, P.J. Tambade, K.D. Bhatte, B.M. Bhanage, Adv. Synth. Catal. 353 (2011) 781–787;
(b) K. Hosoi, K. Nozaki, T. Hiyama, Org. Lett. 4 (2002) 2849–2851.
[14] (a) S. Ding, N. Jiao, J. Am. Chem. Soc. 133 (2011) 12374–12377;
(b) L. Zhang, P. Lu, Y. Wang, Org. Biomol. Chem. 13 (2015) 8322–8329;
(c) S. Ushijima, K. Moriyama, H. Togo, Tetrahedron 68 (2012) 4588–4594.
[15] X. Chen, X.-S. Hao, C.E. Goodhue, J.-Q. Yu, J. Am. Chem. Soc 128 (2006) 6790–6791.
[16] J. Kim, S. Chang, J. Am. Chem. Soc. 132 (2010) 10272–10274.
[17] (a) J. Kim, J. Choi, K. Shin, S. Chang, J. Am. Chem. Soc. 134 (2012) 2528–2531;
(b) K.V.V.K. Mohan, N. Narender, S.J. Kulkarni, Tetrahedron Lett. 45 (2004) 8015–8018;
(c) J. Kim, H. Kim, S. Chang, Org. Lett. 14 (2012) 3924–3927;
(d) J. Xiao, Q. Li, T. Chen, L.B. Han, Tetrahedron Lett. 56 (2015) 5937–5940.
[18] (a) X. Ren, J. Chen, F. Chen, J. Cheng, Chem. Commun. 47 (2011) 6725–6727;
(b) G. Zhang, X. Ren, J. Chen, M. Hu, J. Cheng, Org. Lett. 13 (2011) 5004–5007.
[19] (a) Z. Zhang, L.S. Liebeskind, Org. Lett. 8 (2006) 4331–4333;
(b) P. Anbarasan, H. Neumann, M. Beller, Chem. Eur. J. 16 (2010) 4725–4728;
(c) P. Anbarasan, H. Neumann, M. Beller, Angew. Chem. Int. Ed. 50 (2011) 519–522;
(d) Y. Yang, Y. Zhang, J. Wang, Org. Lett. 13 (2011) 5608–5611.
[20] (a) J. Kim, S. Chang, J. Am. Chem. Soc. 132 (2010) 10272–10274;
(b) J. Kim, H. Kim, S. Chang, Org. Lett. 14 (2012) 3924–3927;
(c) J. Kim, J. Choi, K. Shin, S. Chang, J. Am. Chem. Soc. 134 (2012) 2528–2531;
(d) Z. Wang, S. Chang, Org. Lett. 15 (2013) 1990–1993;
(e) A.B. Pawar, S. Chang, Chem. Commun. 50 (2014) 448–450;
(f) J. Kim, H.J. Kim, S. Chang, Eur. J. Org. Chem. (2013) 3201–3213;
(g) J. Kim, H.J. Kim, S. Chang, Angew. Chem. Int. Ed. 51 (2012) 11948–11959.
[21] R. Kishore, J. Yadav, B. Venu, A. Venugopal, M.L. Kantam, New J. Chem. 39 (2015) 5259–5264.
[22] B. Venu, B. Vishali, G. Naresh, V.V. Kumar, M. Sudhakar, R. Kishore, J. Beltramini, M. Konarova, A. Venugopal, Catal. Sci. Technol. 6 (2016) 8055–8062.
[23] (a) D. Dyker, Handbook of C-H Transformation, vol 1, Wiley-VCH, Weinheim, 2005;
(b) J.-Q. Yu, Z.-J. Shi, C-H Activation, Springer-Verlag, Berlin Heidelberg, 2010.
[24] (a) C.S. Yeung, V.M. Dong, Chem. Rev. 111 (2011) 1215–1292;
(b) J.L. Bras, J. Muzart, Chem. Rev. 111 (2011) 1170–1214;
(c) C.J. Scheuermann, Chem. Asian J. 5 (2010) 436–451;
(d) S.A. Girard, T. Knauber, C.-J. Li, Angew. Chem. Int. Ed. 53 (2014) 74–100.
[25] G. Yan, C. Kuang, Y. Zhang, J. Wang, Org. Lett. 12 (2010) 1052–1055.
[26] A. Khorshidi, Chin. Chem. Lett. 23 (2012) 903–906.
[27] M. Chaitanya, P. Anbarasan, J. Org. Chem. 80 (2015) 3695–3700.
[28] Y. Yang, Y. Zhang, J. Wang, Org. Lett. 13 (2011) 5608–5611.
[29] M. Zhao, W. Zhang, Z. Shen, J. Org. Chem. 80 (2015) 8868–8873.
[30] W.J.J. Stevens, K. Lebeau, M. Mertens, G.V. Tendeloo, P. Cool, E.F. Vansant, J. Phys Chem. B 110 (2006) 9183–9187.
[31] F. Zhang, Y. Yan, H. Yang, Y. Meng, C. Yu, B. Tu, D. Zhao, J. Phys. Chem. 109 (2005) 8723–8732.
[32] N. Rahmat, A.A. Zuhairi, A.A.R. Mohamed, Am. J. Appl. Sci. 7 (2010) 1579–1586.
[33] V. Subbaramaiah, V.C. Srivastava, I.D. Mall, J. Hazard. Mater. (2013) 355–363.
[34] V. Subbaramaiah, V.C. Srivastava, I.D. Mall, AIChE. J. 59 (2013) 2577–2586.
[35] E.S. Sankar, G.V.R. Babu, K. Murali, B.D. Raju, K.S.R. Rao, RSC Adv. 6 (2016) 20230–20239.

[36] D.Y. Zhao, J.L. Feng, Q.S. Huo, N. Melosh, G.H. Fredrickson, B.F. Chmelka, G.D. Stucky, Science 279 (1998) 548–552.
[37] G. Saidulu, N. Anand, K.S. Rama Rao, B. Abhishek, S.E. Park, B.D. Raju, Catal. Lett. 141 (2011) 1865–1871.
[38] V. Subbaramaiah, V.C. Srivastava, I.D. Mall, Ind. Eng. Chem. Res. 52 (2013) 9021–9029.
[39] H. Knozinger, P. Ratnasamy, Catal. Rev. 17 (1978) 31–70.
[40] N. Scotti, M. Dangate, A. Gervasini, C. Evangelisti, N. Ravasio, F. Zaccheria, ACS Catal. 4 (2014) 2818–2826.
[41] V. Chaudhary, Sweta, Int. J. Sci. Eng. Res. 7 (2016) 1743–1748.
[42] L.F. Chen, P.J. Guo, L.J. Zhu, M.H. Qiao, W. Shen, H.L. Xu, K.N. Xu, Appl. Catal. A: Gen. 356 (2009) 129–136.
[43] X. Guo, A. Yin, W.L. Dai, K. Fan, Catal. Lett. 132 (2009) 22–27.
[44] M.K. Chahal, M. Sankar, RSC Adv. 5 (2015) 99028–99036.
[45] Y. Zhu, M. Zhao, W. Lu, L. Li, Z. Shen, Org. Lett. 17 (2015) 2602–2605.